JOURNAL
of
ELECTROANALYTICAL CHEMISTRY
and
INTERFACIAL ELECTROCHEMISTRY

AN INTERNATIONAL JOURNAL DEVOTED TO ALL ASPECTS OF ELECTRODE KINETICS, INTERFACIAL STRUCTURE, PROPERTIES OF ELECTROLYTES, COLLOID AND BIOLOGICAL ELECTROCHEMISTRY

VOL. 69 1976

ELSEVIER SEQUOIA S.A.

LAUSANNE

J. Electroanal. Chem., 69 (1976) 317—338

STUDY OF PLATINUM ELECTRODES BY MEANS OF THIN LAYER ELECTROCHEMISTRY AND LOW-ENERGY ELECTRON DIFFRACTION

PART I. ELECTRODE SURFACE STRUCTURE AFTER EXPOSURE TO WATER AND AQUEOUS ELECTROLYTES

ROY M. ISHIKAWA and ARTHUR T. HUBBARD

Department of Chemistry, University of Hawaii, Honolulu, Hawaii 96822 (U.S.A.)

(Received 21st August 1975)

ABSTRACT

Thin layer electrochemistry (t.l.e.) was combined with low-energy electron diffraction (l.e.e.d.) in order to study the relationship between electrochemical reactivity and the structure of the electrode surface with an adsorbed layer of electrolyte. Atomically clean Pt(100) single crystal electrode surfaces were prepared and characterized by means of l.e.e.d. and a.e.s. The elemental composition of the interface was monitored by means of a.e.s., at a sensitivity of about 1% of a monolayer toward significant surface contaminants, after each stage of the experiment, so as to verify the absence of accidental contamination throughout the procedure. An adsorbed layer remains on the Pt(100) surface after treatment with liquid H_2O or vapor. This layer gives well defined l.e.e.d. patterns, indicating that the metal surface has reconstructed from the [$\sqrt{29} \times \sqrt{170}, 111.8°$] R 4.4° symmetry observed before exposure to the simpler [1 × 1] surface. Treatment of the surface with 1 *M* $HClO_4$ gave a similar l.e.e.d. pattern, but with more evidence of diffuse scattering by the adsorbed layer, and strong a.e.s. signals for the elements Cl and O.

INTRODUCTION

Direct experimental information as to the structure of a surface can be obtained by means of low-energy electron diffraction, l.e.e.d. [1—3]. The elemental composition of the surface can be determined by means of Auger electron spectroscopy, a.e.s. [4—6], performed with the same apparatus as l.e.e.d. [7]. By combining techniques such as l.e.e.d. and a.e.s. with the electrochemical techniques it is possible to determine the structure of an electrode surface before and after exposure to an electrolytic solution [8]. Described here are initial experiments of this type in which the structure and composition of a Pt(100) surface has been determined by means of l.e.e.d. and a.e.s. prior to and following treatment with H_2O vapor, liquid H_2O, 1 *M* HCl or 1 *M* $HClO_4$. The (100) surface of Pt was chosen over other Pt surfaces, as the one to be studied first, because it forms an ordered surface when clean which undergoes interesting structural rearrangements under the influence of adsorption [9].

Pt electrodes fabricated from single crystals have been studied before. For instance, a skilful study of the voltammetric behavior of crystal surfaces cut parallel to the (100), (111) and (110) planes of Pt has been described [10]. However, at that time the technology for direct determination of electrode surface structure was not available, and results obtained since then indicate that in those experiments the electrode surface structure was unknown and continually changing. For instance, most, if not all, electrolytic ions and solvents adsorb on the Pt surface [11—14]. Indeed, the extensive literature of studies performed by means of ultra-high vacuum techniques indicates that Pt reacts with all but the most inert reagents at pressures below 10^{-6} Torr to form a new surface structure or a disordered layer [1,15]. Further, surfaces of most crystallographic orientations, even when scrupulously cleaned, exhibit structures different from the crystallographic plane to which they are parallel [16]; in particular, the (100) face of Pt, when atomically clean, adopts a structure very different from the ideal crystallographic plane [9].

There is ample evidence that the reactivity of Pt electrodes depends critically upon structural features related, in an unknown way, to the pretreatment process [17]. Studies of electrode reactivity, in order to be complete, must therefore include determination of surface structure before and after electrolysis by a direct method such as l.e.e.d.

Since no presently available surface crystallographic method can be applied while the surface is immersed in a liquid electrolyte, one is faced with the task of relating the l.e.e.d. results which are obtained under conditions very different from those encountered in electrochemistry. The positions of surface metal atoms such as Pt determined from l.e.e.d. data obtained following electrolysis are expected to be the same as during electrolysis because evaporation of excess solvent from the surface at room temperature is not expected to release sufficient energy by itself to supply the activation energy necessary to promote a surface structural rearrangement of the metal. Thus, it should generally be possible to infer the positions of electrode surface metal atoms, resulting from electrolysis, from l.e.e.d. results obtained after electrolysis. Structural changes resulting from such electrolytic processes as electrodeposition of metals, anodization, anodic deposition (e.g., AgCl), electropolishing, electrosorption and electrocrystallization should be amenable to study, as described below.

Non-metallic species are held on the surface with varying degrees of tenacity [15], and thus the structural stability of electrodeposited layers of such materials during evaporation of excess electrolyte would be expected to vary from case to case. Instances in which the adsorbate reacts chemically with the adsorbent, resulting in coordination, oxidation or reduction, are marked by chemical stability comparable to homogeneous compounds. Surface oxides, halides, sulfides and chemisorbed unsaturated hydrocarbons belong to this category [1]. The stability of non-metallic adsorbed layers of single atoms or small molecules toward electron-bombardment damage is a thousand-fold greater than for the corresponding non-metallic solid [18], presumably due

to an efficient transfer of energy to the metallic substrate [19]. The ability of typical adsorbates to remain adsorbed on the surface after re-evacuation to ultra-high vacuum can be taken as an indication that their surface structures are kinetically stable. Thus, it should be worthwhile to determine the structure of electrosorbed layers of atoms and small molecules by means of l.e.e.d. experiments following electrolysis. The layer of chemisorbed solvent and electrolytic ions remaining on the surface after exposure to an inert liquid electrolyte belongs in this category. In other words, the region of the interface referred to as the "compact layer" in the electrochemical parlance [20] is comparable to the "chemisorbed layer" observed in gas—solid surface research.

The theory and practice of l.e.e.d. have been reviewed recently [1—3]. A brief account will be given here. Electrons are directed onto a polished metal surface in a 1 μA collimated beam of about 1 mm diameter at an accurately-known angle near normal incidence. Two angles, defined by Fig. 1, must be specified: the angle of incidence measured with respect to the surface normal (the "rocking angle", θ_i); and the angle of rotation about the surface normal with respect to a specified surface unit mesh vector (the "azimuthal angle", ϕ) [21]. About 99% of the electrons lose energy to interactions with electrons of the solid and re-emerge in all directions. The remaining 1% emerge, without loss of energy, in directions related to the sample surface atomic structure. The surface sensitivity of l.e.e.d. arises from the fact that the mean free path (MFP) of low-energy (20 to 200 eV) electrons is on the order of atomic dimensions, given approximately by eqn. (1) [1],

$$\text{MFP} \approx 1 + (V_p/150)^2 \tag{1}$$

if MFP is expressed in Å units and the energy, V_p, of electrons in the incident

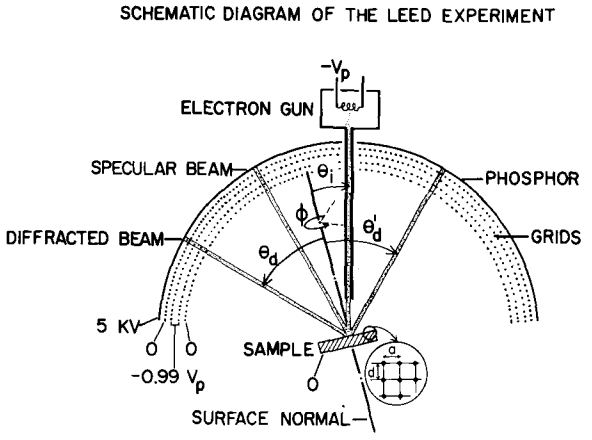

Fig. 1. Schematic diagram of the l.e.e.d. experiment. Incident beam parameters: "rocking angle", θ_i, "azimuthal angle", ϕ, incident beam energy, V_p. Diffracted beam parameters: angles of diffraction, θ_d and θ_d', interrow lattice spacing, a, interlayer lattice spacing, d, as defined in Figure and text.

beam in electron volts (eV). A series of four closely-spaced, concentric, spherical grids are interposed between the sample and the phosphorescent display screen. The first and fourth grids are at ground potential to prevent distortion of the l.e.e.d. pattern by the retarding potential (about $-0.99\ V_p$) of the second and third grids and the high voltage of the phosphorescent screen. Only the elastically scattered electrons contribute to the observed pattern of spots on the phosphorescent screen. The direction of the diffracted beam is determined by the fact that the elastically-scattered intensity is appreciable only when rays from all scattering centers emerge in phase, a requirement which can be written relatively simple in two dimensions, eqns. (2) and (3),

$$m\lambda = a(\sin\theta_d \pm \sin\theta_i) \tag{2}$$

$$\lambda = (150.4/V_p)^{1/2} \tag{3}$$

where λ is the de Broglie wavelength of the incident electron in Å, and $m = 0$, 1, 2, ... A lucid, three-dimensional treatment, in vector notation, is given in ref. 22. Were it not for the fact that elastically scattered electrons typically are scattered more than once before emerging, the incident energies at which maximum intensity occurs would have corresponded to the Bragg condition for constructive interference of scattered rays from various depths within the sample, eqn. (4);

$$m\lambda = d(\cos\theta_d + \cos\theta_i) \tag{4}$$

but instead, as a result of multiple scattering, the intensity varies in a more compicated way as the sum of the intensities scattered from each atom in the sample. In writing each term of the summation, account must be taken of the energy- and direction-dependence of the elastic scattering cross-section of each center, of the attenuation due to inelastic scattering along the actual path followed by each ray, and of the phase angle (position and direction) of each ray such that out-of-phase rays cancel.

In practical terms, the meaning of eqns. (1)—(4) is:

(i) that the non-specular beams converge on the specular beam and beams of higher order, m, become visible as the incident energy, V_p, increases;

(ii) that the intensity of each diffracted beam fluctuates as V_p is varied; the various beams achieve their intensity maxima at approximately the same energies;

(iii) that the symmetry of the l.e.e.d. pattern defines the symmetry of the sample surface.

Point (iii) is illustrated by Fig. 2; a surface having the surface unit mesh defined by the basis vectors a and b will give rise to the l.e.e.d. pattern defined by reciprocal lattice basis vectors A and B. The surface unit mesh can thus be deduced from the l.e.e.d. pattern by using the definition of the reciprocal lattice, eqns. (5) and (6),

$$A = 2\pi(b \times c)/(a \cdot b \times c) \tag{5}$$

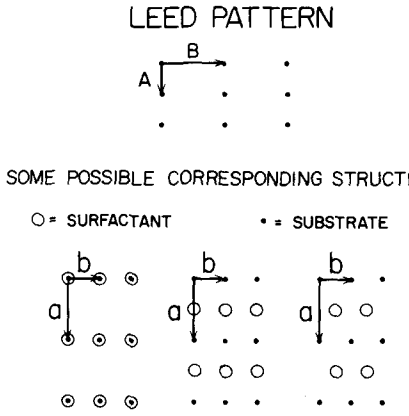

Fig. 2. Some different surface structures producing equivalent l.e.e.d. patterns.

$$B = 2\pi(a \times c)/(b \cdot a \times c) \tag{6}$$

in which c is a unit vector perpendicular to the surface; after finding the scalar products in eqns. (7) and (8),

$$a \cdot A = b \cdot B = 2\pi \tag{7}$$

$$a \cdot B = b \cdot A = 0 \tag{8}$$

it is evident that a is perpendicular to B, as is b to A, and that the lengths of A and B are reciprocally related to the lengths of a and b, respectively. However, the *structure* of the surface commonly cannot be inferred conclusively from the *symmetry* because there may be numerous plausible structures corresponding to a given lattice symmetry, as illustrated in Fig. 2; surface crystallographic analysis of accurate intensity—energy data allow the correct structure to be identified, at least in favorable cases [21].

Auger electron spectroscopy (a.e.s.) is the most effective of the alternative methods for elemental analysis of monolayers on solids in connection with l.e.e.d. experiments because it can be performed simply with the use of the l.e.e.d. optics [7]. There is a burgeoning literature of such applications of a.e.s., including several excellent reviews [4—6]. Only a brief review of a.e.s. as applied to these studies will be given here. In a.e.s. experiments a 10 μA beam of electrons of kinetic energy about 2000 eV is directed onto the sample at a glancing angle of about 17° from the surface plane, causing ionization of atoms in the surface region. One ionization event out of about 10^4 produces an Auger electron which emerges from the sample without losing energy to inelastic scattering processes in the sample. The Auger electron kinetic energy, eqn. (9),

$$\text{Auger electron energy} = E_w - E_x - E_y - \phi_w(s) + \phi_w(a) \tag{9}$$

equals the binding energy of the electron initially removed, E_w, less that of the "down" electron, E_x, captured by the initially-ionized level, and the "up" electron, E_y, ejected from the sample, corrected for the work functions of the sample, ϕ_w(s), and analyzer, ϕ_w(a). Thus, the Auger electrons from atoms which compose the electrode surface region are emitted with widely separated energies characteristic of the individual elements which are present. All elements except H and He emit Auger electrons. The Auger electron yield from a superficially adsorbed layer is proportional to surface coverage [23], but the proportionality constant must be obtained by means of a calibration experiment with the same or very similar surfactant adsorbed at known coverage on the same substrate [25], eqn. (10),

$$ {}_jI_a - I_s(E_j) \exp\left[1 - \sum_k \Gamma_k Q_k(E_j)\right] = I_p K(\sin\theta_2 - \sin\theta_1) G_j \Gamma_j \approx {}_jI_a \qquad (10) $$

where the symbols are as follows: $K(\sin\theta_2 - \sin\theta_1)$ = collection efficiency of electron analyzer (ref. 25); ${}_jI_a$ = Auger electron current due to element j (A); G_j = proportionality constant appropriate to j; Γ_k = interfacial concentration of species k, (mol cm^{-2}); $I_s(E_j)$ = the substrate current detected at the kinetic energy of E_j, in the absence of the adsorbed layer (A); $Q_k(E_j)$ = molar cross-section for inelastic scattering of Auger electrons of energy E_j by species k (cm^2 mol^{-1}); I_p = incident beam current (A).

The exponential term makes a small adjustment in the background Auger electron emission from the substrate for partial attenuation by the adsorbed layer. The approximate form of eqn. (10) is usually adequate because background corrections are frequently small. Since the Auger electrons are a small fraction of the total current it is necessary to differentiate the signal in order to clearly distinguish the Auger signal from the larger but more gradually varying scattered electron signal (dI/dE is obtained electronically). The total Auger electron current, ${}_jI_a$, is computed from the derivative of the electron energy distribution curve, $N'(E) \equiv dI/dE$, on the assumption that the distribution is Gaussian, by taking the first derivative of the equation defining the Gaussian distribution. The result is given by eqn. (11),

$$ I_a = (32\pi e)^{1/2}(\sigma^2/k^2)A_2 \qquad (11) $$

where σ is the standard deviation of the Gaussian, k is the modulation amplitude (V), and A_2 is the maximum amplitude of the $N'(E)$ curve in the negative direction. The magnitude of σ is found by noting the energy, E_{peak}, at which $N'(E)$ crosses zero and the energy, $E_{peak} + \sigma$, at which $N'(E)$ achieves its negative maximum, A_2. Measurement of A_2 at the negative rather than the positive maximum takes advantage of the fact that the Auger electron energy distribution is most nearly ideal on that (high-energy) side of the peak; interaction of the Auger electron with the valence and conduction electrons of the sample interferes with the spectrum on the low-energy side.

The subject of electrochemistry with thin layer electrodes was reviewed re-

cently [8,24]. A principle advantage of t.l.e. for surface studies of this type is that the volume of solution contacting a square centimeter of the electrode area during each trial is only 10^{-3} cm^3; accordingly, the amount of reactant present in a surface monolayer (about 2×10^{-9} mol cm^{-2}) is comparable to the amount in solution (about 1×10^{-9} mol cm^{-2} assuming a concentration equal to 1×10^{-3} M). This circumstance facilitates detection of adsorbed reactants and helps to prevent contamination of the surface. In fact, Auger electron spectra of the Pt(100) surface obtained after exposure to the argon atmosphere and various aqueous solutions indicated the absence of significant accidental contamination. This paper deals only with a few basic experiments intended to pave the way for more inclusive future studies in which the advantages of t.l.e., already demonstrated with conventional polycrystalline electrodes, will be exploited with electrodes of well-defined structure, purity and composition for investigation of reaction stoichiometry, electrode kinetics, chemical reactions coupled to electrode reactions, and, particularly, surface-related processes such as electrodeposition, electrosorption and surface oxidation/reduction [8].

RESULTS AND DISCUSSION

The clean Pt(100) surface exhibits the characteristically complex l.e.e.d. pattern described by other workers [9,26—30], (Fig. 3). The l.e.e.d. pattern of an ideal (100) face of a face-centered cubic metal such as Pt would be a square array of spots located where the corners of the squares appear in the pattern of Fig. 3. These "ideal" spots are visible in Fig. 3, but a large number of additional spots are also visible. In fact, the pattern is composed of two similar arrays of three parallel rows, rotated 90° and superimposed to form squares. Each row is three spots wide and additional spots are faintly visible in some cases. The spacing between groups of three along each row is one-fifth of the interrow spacing, indicating that the surface unit mesh comes into register with the substrate unit mesh once every five substrate atoms; similarly, the spacing between spots is one-thirteenth of the interrow spacing indicating coincidence with the substrate every thirteen atoms. The groups of three are arranged linearly so as to make an angle of 68.2° with the rows and 111.8° with the columns. A schematic diagram of the unit mesh corresponding to each of the two perpendicular arrays [9] is shown in Fig. 4. The positions of atoms within the unit mesh is unknown, pending surface crystallographic refinement of l.e.e.d. relative intensity data. If the conventional nomenclature [1] were generalized to allow for an angular orientation of the unit mesh vectors in the coated surface different from that of the substrate, this surface would be denoted, Pt(100) [$\sqrt{170} \times \sqrt{29}$, 111.8°] R 4.4°, where $\sqrt{170}$ and $\sqrt{29}$ are the lengths of the surface unit mesh vectors expressed as multiples of the substrate unit mesh, 111.8° is the angle between these vectors, and R 4.4° signifies that the $\sqrt{170}$ vector is rotated 4.4° with respect to the substrate unit mesh.

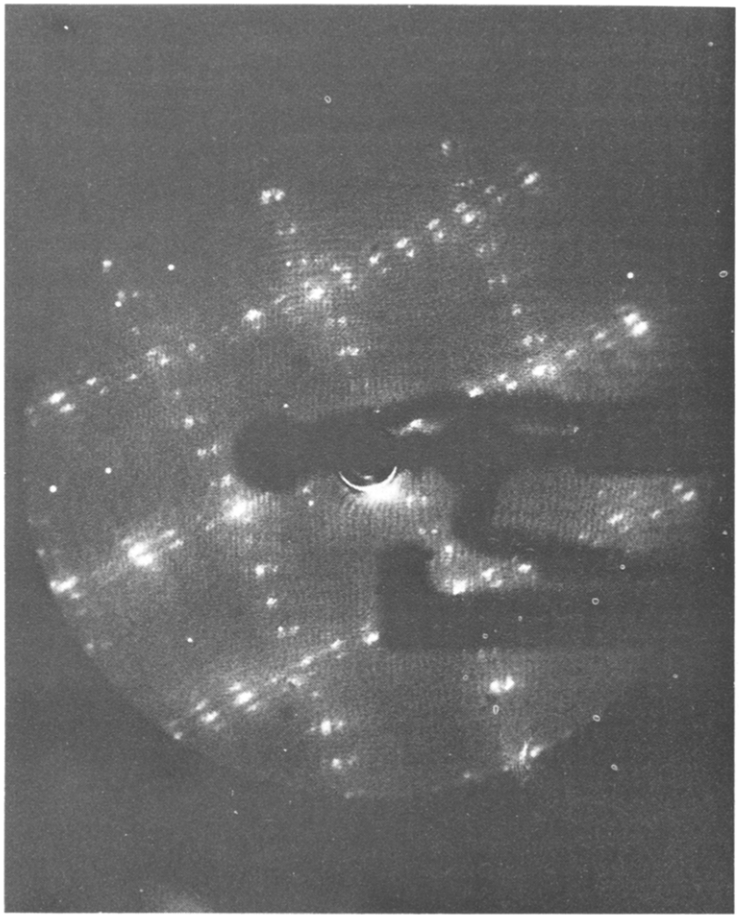

Fig. 3. L.e.e.d. pattern of clean Pt(100) surface. Experimental conditions: incident beam energy, 122 eV; current, 1.6 μA. Camera aperture, f 5.6; exposure, 60 s. Film, Kodak 2475 (ASA 1000).

Auger electron spectra of the clean Pt(100) surface are shown in Fig. 5. Only peaks assignable to Auger transitions among the M, N and O levels of Pt [31] are evident in the spectra, in agreement with Auger spectra of clean Pt reported by Palmberg [9] and Gland and Somorjai [32]. Based upon absolute calibration of the Auger spectrometer for chemisorbed molecular layers, the surface conditions of C, N and O are less than 1.2×10^{13}, 2×10^{13} and 5×10^{13} atoms cm^{-2}, respectively (which correspond to 1, 2 and 5% of a monolayer). Carbon, when it is present, gives rise to a peak at 272 eV (peak energies here refer to the position of the negative inflection of the Auger electron distribution, $N(E)$, which gives rise to the negative-going peaks evident

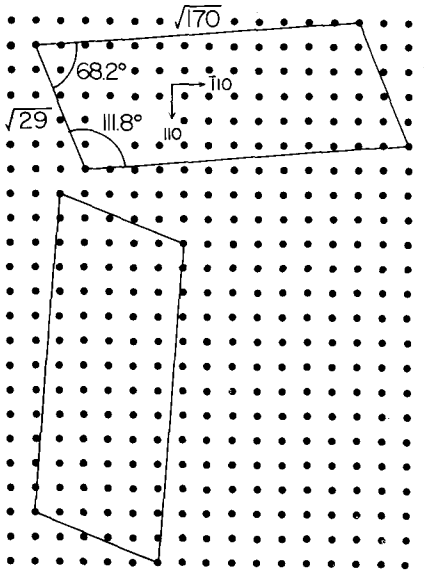

Fig. 4. Unit mesh of the clean Pt(100) surface (parallelogram) in relation to lattice points of the (100) plane of the substrate (dots).

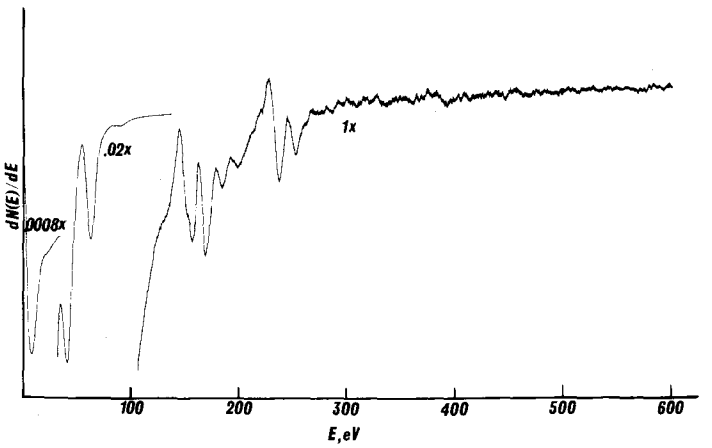

Fig. 5. Auger electron spectra of clean Pt(100) surface. Experimental conditions: incident beam energy, 2000 eV; current, 10 μA. Angle of incidence, θ, measured from the surface plane, 17°; azimuthal angle ϕ (rotation about the surface normal), measured from the [110] zone, 28°. Modulation voltage, 10 V peak-to-peak.

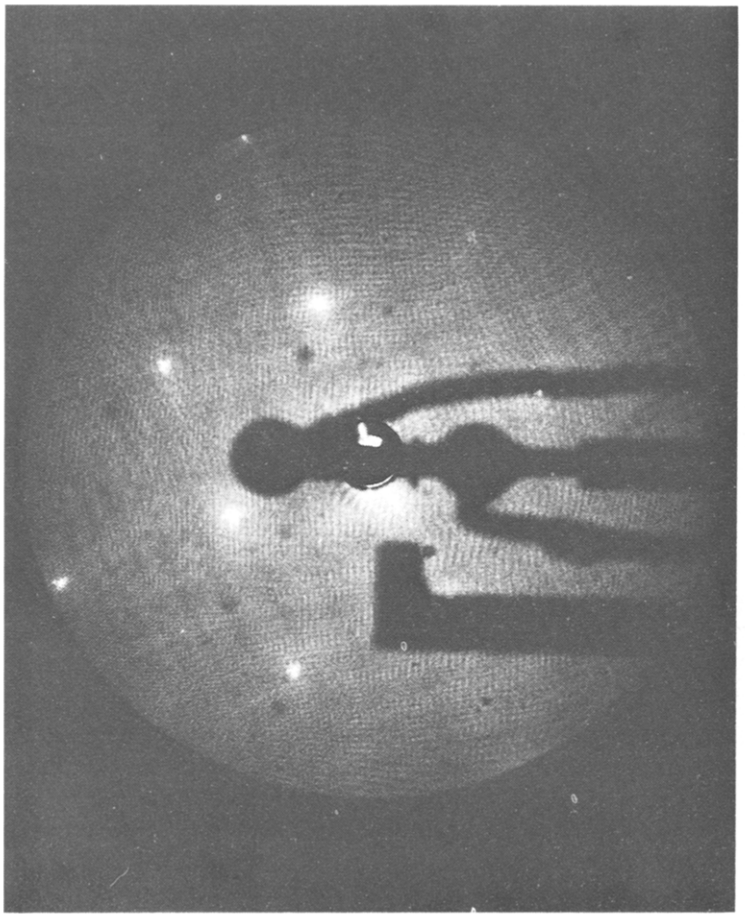

Fig. 6. L.e.e.d. pattern of Pt(100) surface after treatment with liquid H_2O. Experimental conditions: incident beam energy, 125 eV. Other conditions as in Fig. 3.

in derivative plots, $N'(E)$, such as is shown in Fig. 5); N or O if present would give rise to triplets of peaks with the strongest peak at 385 eV or 517 eV, respectively.

The l.e.e.d. pattern obtained for the Pt(100) surface after exposure to liquid water for a period of 120 s at room temperature, followed by re-evacuation, appears in Fig. 6, from which it can be seen that water causes the surface to rearrange to a structure having the square symmetry of an ideal (100) plane of the Pt crystal. This surface contains a layer of chemisorbed H_2O, or fragments derived from H_2O, as can be seen from the Auger electron spectrum appearing in Fig. 7. The peak (negative maximum of $N'(E)$) at 517 eV, one of a triplet of peaks near 500 eV assignable to oxygen [31], indicates the pres-

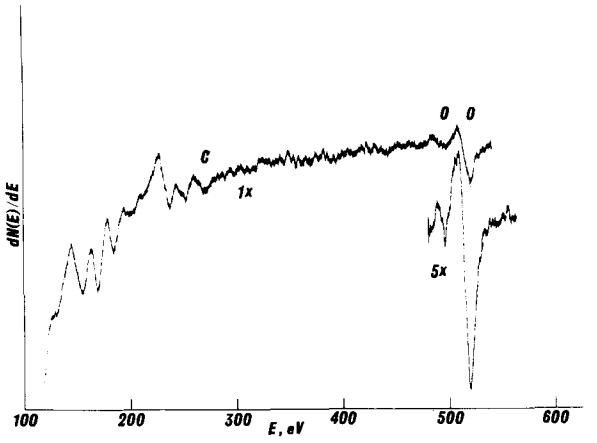

Fig. 7. Auger electron spectra of Pt(100) surface after treatment with liquid H_2O. Experimental conditions: incident beam energy, 1500 eV. Other conditions identical to those of Fig. 5.

ence of about 10^{15} atoms cm^{-2} of the element oxygen [25] (there are 1.3×10^{15} Pt atoms cm^{-2} of the ideal Pt(100) surface). This represents a lower limit of the number of H_2O molecules occupying the surface when in contact with liquid water, because partial desorption may occur upon evacuation. The adsorbed layer has the stoichiometry H_2O, based upon mass spectrometric observation of the material which desorbs from the surface upon rapid heating (300, 600 and 900° C). Information regarding the molecular structure of the adsorbed material is being sought [33] by means of electron stimulated desorption and mass spectrometry [18].

Graphs of the specular beam intensity vs. the beam energy (*I—E* curves) for the clean and liquid-water-treated Pt(100) surfaces appear in Fig. 8, from which it can be seen that the efficiency of elastic scattering of electrons in the specular direction is comparable in both cases. Therefore, the scattering centers (surface metal atoms and adsorbed molecules) must lie in parallel planes. In addition, the maximum intensities of the non-specular beams, such as (10) and (11) (Figs. 3 and 6) are comparable for the clean and coated surfaces, indicating that the layer is ordered in register with the Pt(100) substrate and possesses a square unit mesh. The question as to how the individual molecule within the layer is situated in relation to the metal surface unit mesh, must await future study. For now, this surface will be denoted Pt(100) [1 × 1]-H_2O, in keeping with accepted notation [1].

The Auger spectrum of the Pt(100) [1 × 1]-H_2O surface (Fig. 7) reveals the presence of a very small amount (2×10^{13} atoms cm^{-2}) of carbon. This amount of carbon does not account for the observed change in l.e.e.d. pattern because surfaces containing this amount of carbon but no H_2O display essentially the same l.e.e.d. pattern and *I—E* curve as the clean surface.

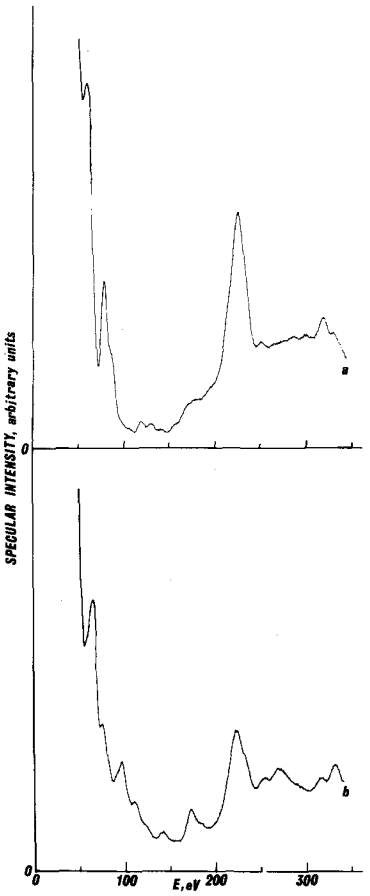

Fig. 8. Intensity of the specularly reflected beam vs. incident beam energy (specular I—E curves) for clean and liquid-water-treated Pt(100) surfaces. (A) Clean surface, (B) liquid-water-treated surface, Pt(100) [1 × 1]-H_2O. Experimental conditions: incident beam current normalized to 0.5 μA; angle of incidence from the surface normal, 4.0°; azimuthal angle from the [110] zone, 28°; acceptance angle of the spot photometer, 0.33°.

When the clean Pt(100) surface was exposed to H_2O vapor, appreciable adsorption was evident from l.e.e.d. patterns and a.e.s. spectra as the H_2O pressure reached 10^{-5} Torr. After 5 min at 10^{-5} Torr the l.e.e.d. pattern changed from the complicated clean-surface pattern, Pt(100) [$\sqrt{170} \times \sqrt{29}$, 111.8°] R 4.4°-$H_2O$, to a simple Pt(100) [1 × 1]-H_2O pattern (Fig. 9). The l.e.e.d. patterns for surfaces exposed to water vapor were the same as those for surfaces treated with liquid water except for a slight increase in the background intensity due to diffuse, elastically-scattered electrons. Perhaps the coverage resulting from exposure to the vapor is slightly less complete than that pro-

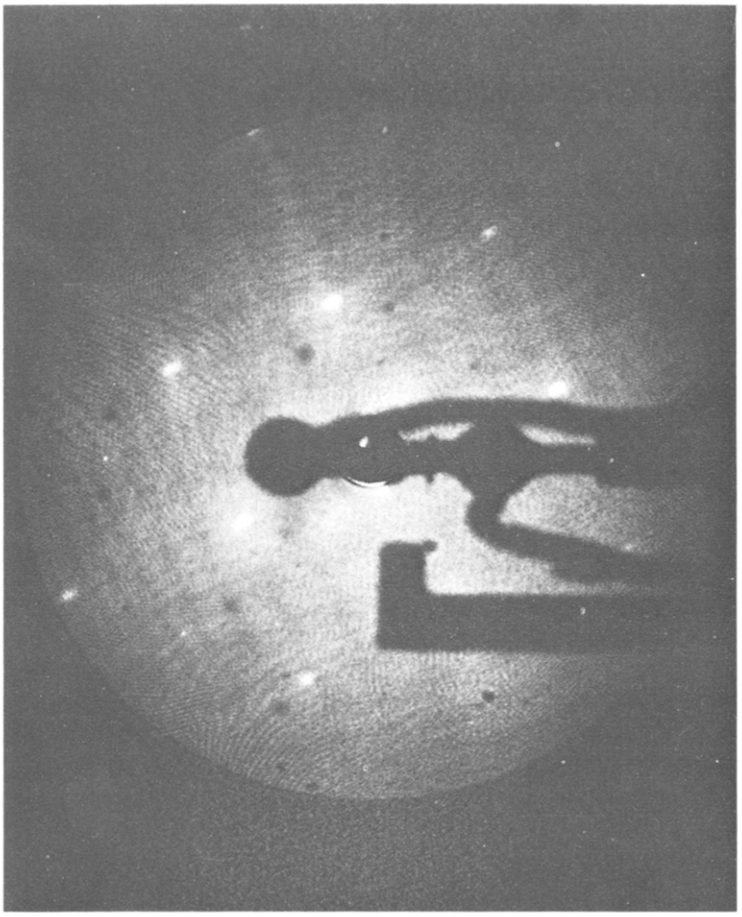

Fig. 9. L.e.e.d. pattern of Pt(100) surface after exposure to water vapor. Experimental conditions: incident beam energy, 122 eV; beam current, 2.1 μA. Pressure of water vapor, 10^{-5} Torr; exposure time, 300 s. Other conditions as in Fig. 3.

duced by liquid H_2O, accounting for a slight increase in the disorder. The Auger spectrum obtained after exposure to H_2O vapor indicates the presence of about 10^{15} atoms cm^{-2} of the element oxygen (Fig. 10). Thermal desorption mass spectrometry indicated that the adsorbed layer had the composition H_2O. The carbon coverage was a factor of three lower than for liquid water, owing to the greater ease of performing the experiment. The *I*—*E* curves (Fig. 11) are similar to those for the liquid-water-treated surface (Fig. 8). Thus, it appears that water forms an ordered layer on the Pt(100) substrate in which the Pt surface and the adsorbed layer both have the same symmetry as an ideal (100) plane.

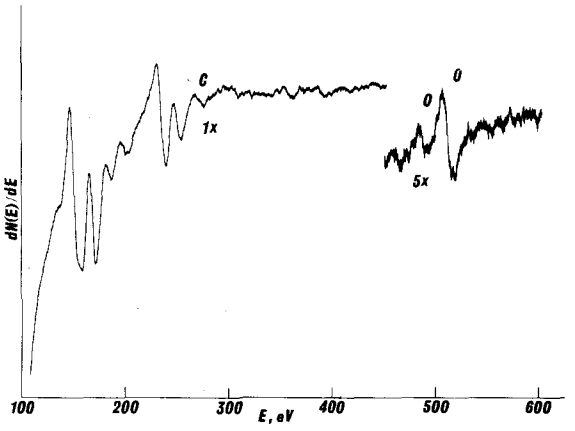

Fig. 10. Auger electron spectra of Pt(100) surface after exposure to water vapor. Experimental conditions: as in Figs. 5 and 9.

A 2 μA incident electron beam 1 mm in diameter represents a flux of one electron per surface atom per second. Thus, there is the distinct possibility of surface alteration due to interaction with energetic electrons, the extent of which will depend on the interaction cross-sections and thermal stability of the adsorbed layer. Typically, these beam-induced changes occur slowly or

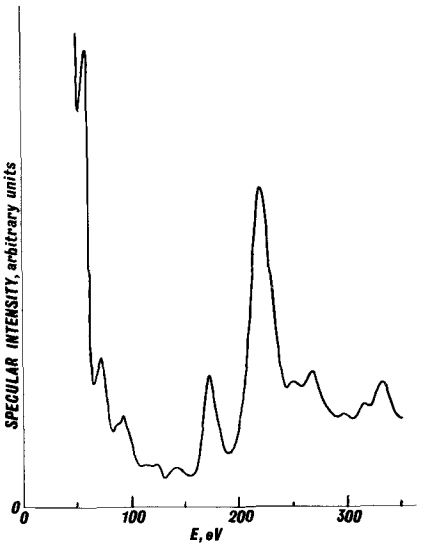

Fig. 11. Specular I—E curve for a water-vapor-treated Pt(100) surface. Experimental conditions: as in Figs. 8 and 9.

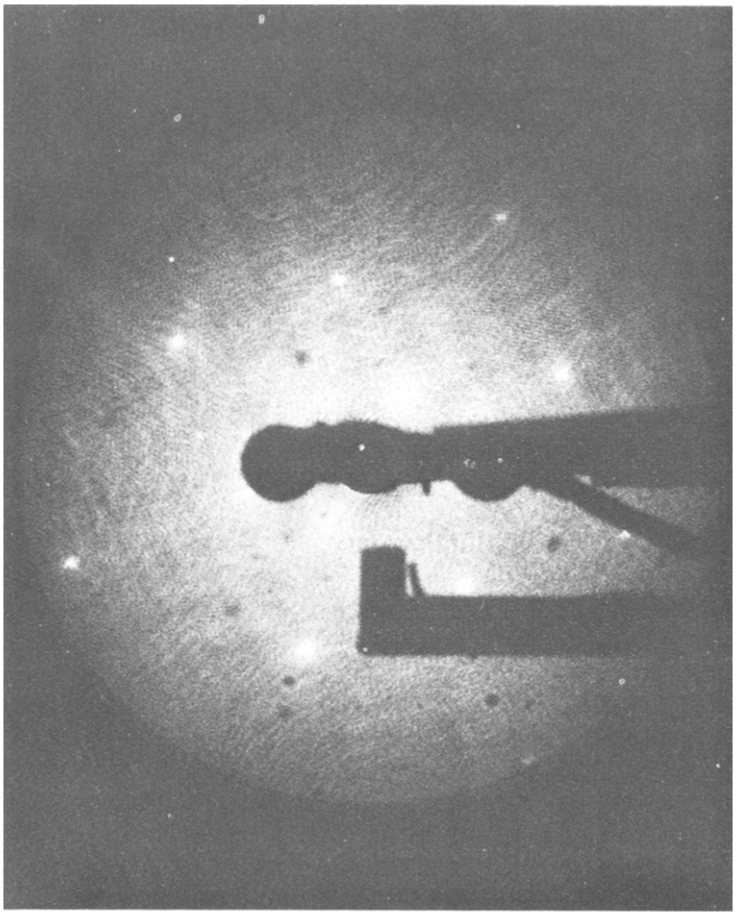

Fig. 12. L.e.e.d. pattern of Pt(100) surface after treatment with 1 *M* HCl. Experimental conditions: incident beam energy, 125 eV; current 1.7 μA. Camera aperture, *f* 8; exposure, 30 s. Other conditions as in Fig. 3.

not at all, allowing reliable l.e.e.d. and a.e.s. characterization to be made although reasonable care must be taken to minimize exposure to the beam. The Auger electron signal due to oxygen adsorbed on the Pt electrode was constant over a period of 15 min under exposure to a 10 μA beam at 2000 eV.

After treatment with 1 *M* HCl the Pt(100) surface exhibited a (1 × 1) l.e.e.d. pattern (Fig. 12). The diffuse scattering is somewhat larger than for surfaces treated with pure water (Fig. 6) indicating a somewhat lesser degree of order. However, the appearance of a Cl peak at 185 eV and the absence of elemental oxygen in the Auger spectrum (Fig. 13) reveals the remarkable result that HCl has completely displaced the H_2O from the surface. It was observed earlier [11] that Cl^- is strongly and irreversibly chemisorbed on Pt

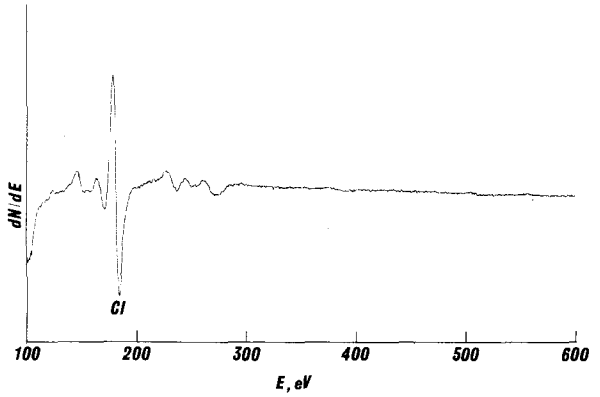

Fig. 13. Auger electron spectrum of Pt(100) surface after treatment with 1 *M* HCl. Experimental conditions: incident beam energy, 2000 eV; current, 50 μA. Other conditions as in Fig. 5.

from aqueous solution, but the displacement of H_2O from the compact layer by Cl^- had not been demonstrated previously.

Treatment of the Pt(100) surface with 1 *M* $HClO_4$ at a potential of 0.405 V versus a calomel electrode prepared with 1 *M* NaCl exhibited a (1 × 1) l.e.e.d. pattern similar to that for 1 *M* HCl. The Auger electron spectrum (Fig. 14) indicates the presence of Cl and O in proportions corresponding to ClO_4^- at a coverage approximating one ClO_4^- per platinum atom. Thus, it is tempting to speculate that the exposure to perchloric acid and the subsequent evaporation process produced a Pt surface having the symmetry of an ideal Pt(100) plane and an ordered overlayer of ClO_4^- ions and H^+ counterions, one pair per Pt surface unit mesh; a more detailed discussion will be left to future articles.

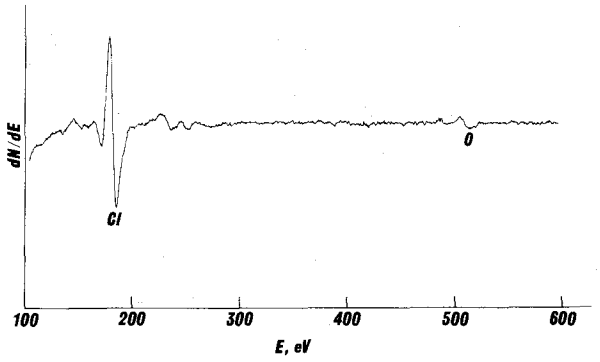

Fig. 14. Auger electron spectra of Pt(100) surface after treatment with 1 *M* $HClO_4$. Experimental conditions: incident beam energy, 2000 V; current, 50 μA. Modulation voltage, 5 V peak-to-peak. Other conditions as in Fig. 5.

EXPERIMENTAL

The sequence of experimental steps was as follows:

(i) Vacuum system baked and all filaments lighted to remove adsorbed gases;

(ii) sample cleaned by heating in oxygen, Ar^+ bombardment and resistance heating;

(iii) Auger electron spectra recorded, using the l.e.e.d. optics as the electron energy analyzer;

(iv) l.e.e.d. patterns obtained;

(v) sample positioned as a thin layer electrode, isolated from l.e.e.d. chamber, and brought to 760 Torr with pure argon;

(vi) electrochemical characterization of sample carried out;

(vii) sample isolation valve re-evacuated and opened;

(viii) post electrochemical l.e.e.d. and Auger electron characterization carried out.

The instrument used for this work [8] was constructed such that the l.e.e.d., a.e.s., m.s., and t.l.e. experiments were carried out without removing the sample from the vacuum chamber (Fig. 15). Transfer of the electrode from one instrument to another would be almost certain to result in contamination. The vacuum system [34] was constructed from ultra-high vacuum materials, primarily stainless steel, and had no moving seals (Varian Associates, Vacuum Division, Palo Alto, Calif. 94303, U.S.A.). Prior to each use, the entire vacuum system was baked at 250° C for 12 h to facilitate removal of volatile materials from the inside surfaces of the apparatus; this was essential to the attainment of the atomically clean electrode surface. When the apparatus had cooled to room temperature, the residual pressure was about 1×10^{-10} Torr. The ion gauge and particle gun filaments were then operated at maximum temperature for 30 min to degas the surrounding surfaces. The residual gas consisted of He, C, CH_4, H_2O, CO, N_2, O_2, Ar and CO_2 in molar amounts comparable within an order of magnitude. The system was equipped with a quadrupole mass spectrometer for residual gas analysis (Electronic Associates, Inc., Model 1110A, West Long Branch, N.J. 07764, U.S.A.).

Evacuation was accomplished by means of four separate pumping systems, which were activated at various stages during the experiments:

(i) cryogenically cooled molecular sieves were employed to pump the system from atmospheric pressure to below 10^{-3} Torr (Varian Vac Sorb), in order to avoid pump oil and vibration which are side-effects of most mechanical pumps;

(ii) ionization pumps, in which a magnetically-confined electron flux ionized residual gas particles and a 5 kV electric field propelled these ions into the pump walls (Varian Vac Ion FC12E), served to reduce the pressure from 10^{-3} Torr to the working range, 10^{-10} Torr;

(iii) cryogenically cooled panels were used to selectively pump condensable gases without removing desirable constituents;

(iv) titanium sublimation pumps, consisting of incandescent Mo/Ti alloy fila-

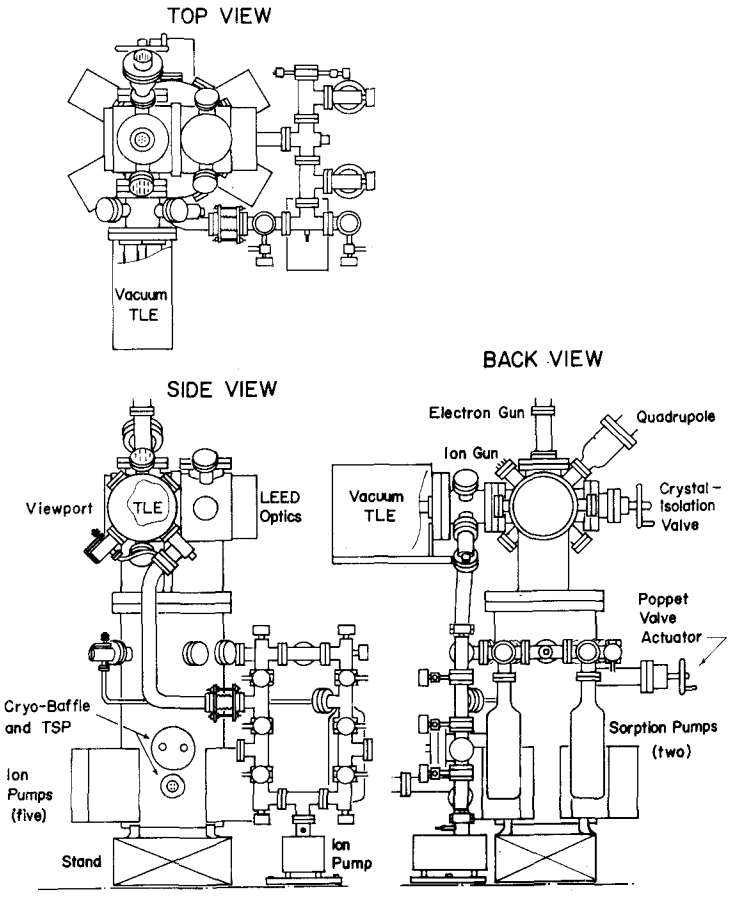

Fig. 15. Sketch of the l.e.e.d.—electrochemistry system.

ments, were utilized to remove reactive gases from Ar by chemisorption onto the freshly-deposited metal film.

L.e.e.d. patterns were obtained by means of optics having four grids, a phosphorescent screen and an electron gun protruding through the center of the screen (Varian 981-0127). The resulting patterns were photographed by means of a camera mounted on a hinged bezel over the viewport (Nikkormat FTN, Nippon Kagaku, Inc., Garden City, N.Y. 11530); cameras designed properly for cloud chamber photography are also suitable.

Auger electron emission was induced by means of an electron gun operating at energies between 500 and 3000 eV and currents between 0 and 100 μA with beam diameters from 0.1 to 1 mm (Varian 981-2454), mounted such that the beam impinged on the sample at glancing incidence (17° from the surface plane), in order to favor excitation of atoms located near the surface.

Auger electron energy distributions were determined by using the l.e.e.d. optics as a retarding-field electron-energy analyzer [7]. A lock-in amplifier was employed to convert the first or second harmonic of the a.c. modulated Auger electron signal to a filtered d.c. signal (Princeton Applied Research, Model 128, Princeton, N.J. 08540) which was graphed by an XY-plotter (Hewlett-Packard Co., Model 7034A, Page Mill Road, Palo Alto, Calif. 94304). A modulation frequency of 10^3 Hz was employed. The energy range covered by the Auger spectrum was scanned over a period of 300 s, corresponding to scan rates less than or equal to 2 V s^{-1}, and the time constant of lock-in amplifier RC filter was 1.0 s. The focal point of the energy analyzer was determined by optimizing the intensity and resolution of the elastically scattered peak.

Electrochemical characterization of the working face of the single crystal sample was accomplished as follows: the sample was positioned in contact with the ends of a pair of Pyrex glass capillaries (1 mm i.d. × 6 mm o.d., Fig. 16). The tips of the capillaries were sealed so as to form a common end with a single opening at its center; a circular recess 0.02 mm deep and 5 mm wide was ground into the tip so that the sample and capillary formed a thin layer cavity. Apart from the tip, the outside of the capillary was coated with pla-

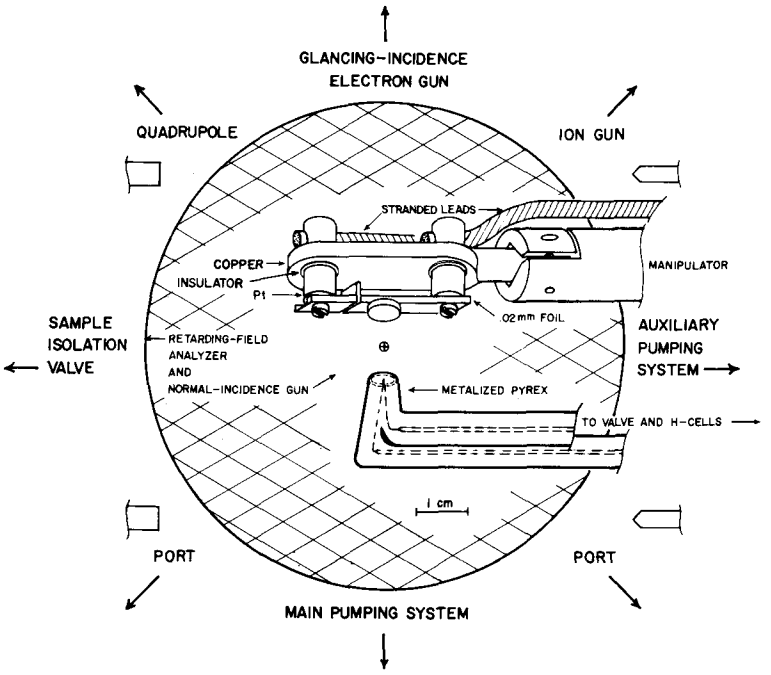

Fig. 16. Sample holder and capillary of the vacuum thin layer electrode system, as seen through the view port of the work chamber, with the l.e.e.d. optics in the background.

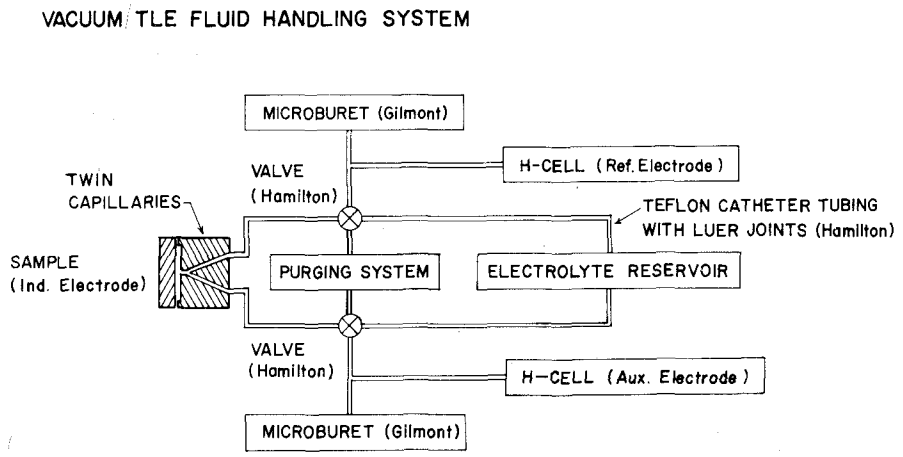

Fig. 17. Schematic diagram of H-cell system used in l.e.e.d./t.l.e. experiments.

tinum to prevent accumulation of charge during l.e.e.d. and a.e.s. experiments. During electrochemical experiments, the sample and capillary were enclosed in a crystal-isolation valve and brought to atmospheric pressure with pure argon by means of an auxiliary vacuum system, described below. Electrolyte was introduced from microburets (Cole-Parmer Instrument Corp., 7425 N. Oak Park Ave., Chicago, Ill. 60648) by means of a system of miniature valves and fittings (Hamilton Co., Reno Nev. 89502, Fig. 17). All fittings were electrically isolated and were constructed so that only inert materials, Teflon, Kel-F, platinum and glass, contacted the solution. In order to prevent introduction of air along with the electrolyte, connection of the microburets to the capillaries was made by means of rod-shaped Kel-F Luer fittings which were mounted in O-ring seals and advanced through an in-line valve (Varian, 951-5052), both sides of the valve having been purged with argon before opening. Connection to the capillaries was made by means of platinum Luer fittings and tubing, which provided the necessary ruggedness and flexibility. The two capillaries were employed to connect the thin layer cavity to the reference and auxiliary electrodes through separate solution paths so as to reduce the contribution of ohmic voltages to the measured electrode potential to a negligible level. A calomel electrode, prepared with 1 *M* NaCl, was the reference half-cell. The spread of Cl^- from the reference electrode into the remainder of the liquid-handling system was carefully avoided in view of the fact that Cl^- adsorbs strongly and irreversibly on Pt electrodes [35].

After completion of the electrolytic stages of each experiment, the isolation valve was evacuated by means of an auxiliary pumping system and opened to the main pumping system (Fig. 18); the pressure was reduced from 760 Torr argon to 2×10^{-9} Torr within about 5 min, such that post-electrochemical

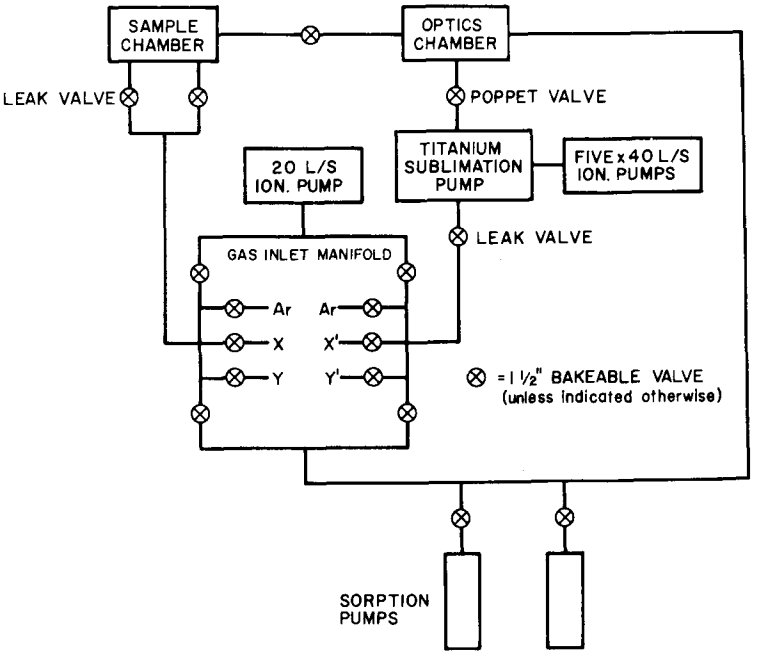

Fig. 18. Schematic diagram of the vacuum system employed for electrochemistry and l.e.e.d.

experiments could begin immediately. At that stage the residual gas was primarily argon, but contained a small fraction of water vapor.

The Pt crystal was cleaned by heating in O_2 for several hours (oxygen pressure, 10^{-7} Torr; sample temperature, 900°C), followed by Ar^+ bombardment at that temperature for one hour (argon pressure, 5×10^{-5} Torr; Ar^+ ion current density, 10 μA cm^{-2}; ion energy, 400 eV), and annealing at 900°C for 3 min. After this cleaning procedure had been applied an Auger electron spectrum over the energy range from 0 to 1000 eV was recorded and if impurities were evident, the ion bombardment was repeated. The details of preparing Pt surfaces free from impurities have been discussed [9,36,37]; in line with previous work, the most persistent impurity on the Pt(100) surface was carbon, attributable to the presence of CO and CH_4 in the residual gas. Electrical power to the ion-pumps was disconnected during Ar^+ ion bombardment to prolong pump life; the purity of the argon was preserved by operating a titanium sublimation filament and an adjoining cryogenically cooled panel, which efficiently removed all chemically reactive impurities, as judged from the mass spectra. Careful cleaning of the ion-bombardment gun (Varian, 981-1045) by electron bombardment heating for 30 min prior to use helped to avoid carbon contamination due to outgassing of the gun.

ACKNOWLEDGMENTS

Acknowledgment is made to the donors of the Petroleum Research Fund, administered by the American Chemical Society, and to the National Science Foundation, for support of this research.

REFERENCES

1 G.A. Somorjai and H.H. Farrell, Adv. Chem. Phys., 20 (1971) 215.
2 P.J. Estrup and E.G. McRae, Surface Sci., 25 (1971) 1.
3 E. Bauer, Techniques Met. Res., 2 (1969) 559.
4 N.J. Taylor, Techniques Met. Res., 7 (1971) 117.
5 C.C. Chang, Surface Sci., 25 (1971) 53.
6 G.A. Somorjai and F.J. Szalkowski, Advances in High Temperature Chemistry, 4 (1971) 137.
7 N.J. Taylor, Rev. Sci. Instr., 40 (1969) 792.
8 A.T. Hubbard, Critical Rev. Anal. Chem., 3 (1973) 201.
9 P.W. Palmberg in G.A. Somorjai (Ed.), The Structure and Chemistry of Solid Surfaces, John Wiley, New York, 1969, p. 29-1.
10 F. Will, J. Electrochem. Soc., 112 (1965) 451.
11 R.F. Lane and A.T. Hubbard, J. Phys. Chem., 77 (1973) 1401.
12 E. Gileadi (Ed.), Electrosorption, Plenum Press, New York, 1967.
13 N.A. Balashova and V.E. Kazarinov, Russian Chem. Rev., Engl. Transl., 34 (1965) 730.
14 R.F. Lane and A.T. Hubbard, J. Phys. Chem., 77 (1973) 1411.
15 G.A. Somorjai and F.J. Szalkowski, J. Chem. Phys., 54 (1971) 389.
16 B. Lang, R.W. Joyner and G.A. Somorjai, Surface Sci., 30 (1972) 440.
17 S.D. James, J. Electrochem. Soc., 114 (1967) 113.
18 T.E. Madey and J.T. Yates, Jr., J. Vac. Sci. Technol., 8 (1971) 525.
19 H. Kuhn, J. Chem. Phys., 53 (1970) 101.
20 P. Delahay, Double Layer and Electrode Kinetics, Interscience, New York, 1965.
21 M.B. Webb and M.G. Lagally, Adv. Solid State Phys., 28 (1973) 301.
22 C. Kittel, Introduction to Solid State Physics, Wiley, New York, 4th edn., 1971, p. 46.
23 R.E. Weber and A.L. Johnson, J. Appl. Phys., 40 (1969) 314.
24 A.T. Hubbard and F.C. Anson in A.J. Bard (Ed.), Electroanalytical Chemistry, Vol. 4, 1971, p. 129.
25 J.A. Schoeffel and A.T. Hubbard, Surface Sci., to be published.
26 A.E. Morgan and G.A. Somorjai, Surface Sci., 12 (1968) 405.
27 A.E. Morgan and G.A. Somorjai, J. Chem. Phys., 51 (1969) 3309.
28 C. Burggrof and A. Mosser, C.R. Acad. Sci., (Paris) 268B (1969) 1167.
29 Y. Berthier, J. Perdereau and J. Oudar, C.R. Acad. Sci. (Paris), 275 C, (1971) 8.
30 T.A. Clarke, R. Mason and M. Tescari, Proc. Roy. Soc. (London), 331A (1972) 321.
31 W.A. Coghlan and R.E. Clausing, Atomic Data, 5 (1973) 317; Surface Sci., 33 (1972) 411.
32 J.L. Gland and G.A. Somorjai, Surface Sci., 38 (1973) 157.
33 B.A. Gordon and A.T. Hubbard, J. Electroanal. Chem., to be published.
34 R.W. Roberts and T.A. Vanderslice, Ultrahigh Vacuum and Its Applications, Prentice-Hall, Englewood Cliffs, N.J., 1963.
35 R.F. Lane and A.T. Hubbard, J. Phys. Chem., 79 (1975) 808.
36 H.B. Lyon and G.A. Somorjai, J. Chem. Phys., 46 (1967) 2539.
37 J.T. Grant and T.W. Haas, Surface Sci., 18 (1969) 457.